SUPPLEMENTAL INFORMATION:

INCREASED FGF21 IN BROWN ADIPOSE TISSUE OF TYROSINE HYDROXYLASE HETEROZYGOUS MICE: IMPLICATIONS FOR COLD ADAPTATION

Patricia Vázquez[1,2,3]*, Catalina Hernández-Sánchez[2,3], Carmen Escalona-Garrido[1,3], Laura Pereira[3,4], Cristina Contreras[5], Miguel López[6,7], Jesús Balsinde[3,4], Flora de Pablo[2,3] and Ángela M. Valverde[1,3]*.

[1]Alberto Sols Biomedical Research Institute (IIBm) (CSIC/UAM), 28029 Madrid, Spain.

[2]Department of Molecular Biomedicine, Centro de Investigaciones Biológicas (CSIC), 28040 Madrid, Spain.

[3]Centro de Investigación Biomédica en Red de Diabetes y Enfermedades Metabólicas (CIBERdem), ISCIII, 28029 Madrid, Spain.

[4]Instituto de Biología y Genética Molecular, Consejo Superior de Investigaciones Científicas (CSIC), Universidad de Valladolid. 47003 Valladolid, Spain.

[5] Physiology Department, Pharmacy School, Complutense University of Madrid, 28040, Madrid, Spain.

[6] NeurObesity Group, Department of Physiology, CIMUS , University of Santiago de Compostela, -Instituto de Investigación Sanitaria , Santiago de Compostela, Spain.

[7]CIBER Fisiopatología de la Obesidad y Nutrición (CIBERobn) , Santiago de Compostela , Spain.

Supplemental Fig. S1

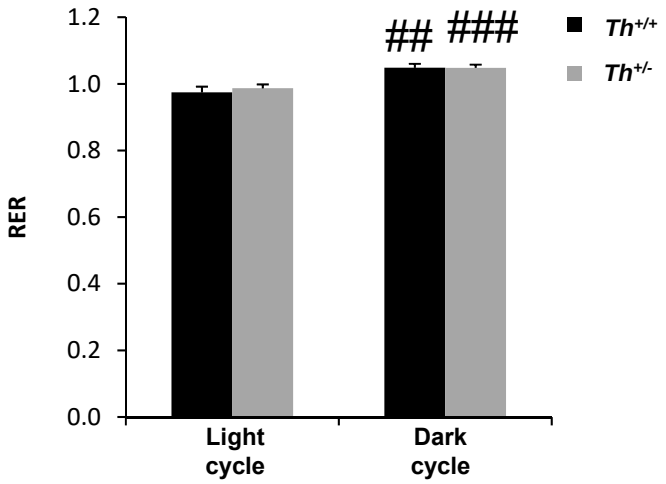

Supplemental Fig. S1. RER analysis at thermoneutrality conditions. Quantification of RER in both genotypes during day and night, at 29ºC. Data are mean ± SEM. n= 7-9/group. Mann–Whitney *U* test was used. $^{\#\#}p<0.01$, $^{\#\#\#}p<0.001$ between each genotype at dark cycle and light cycle.

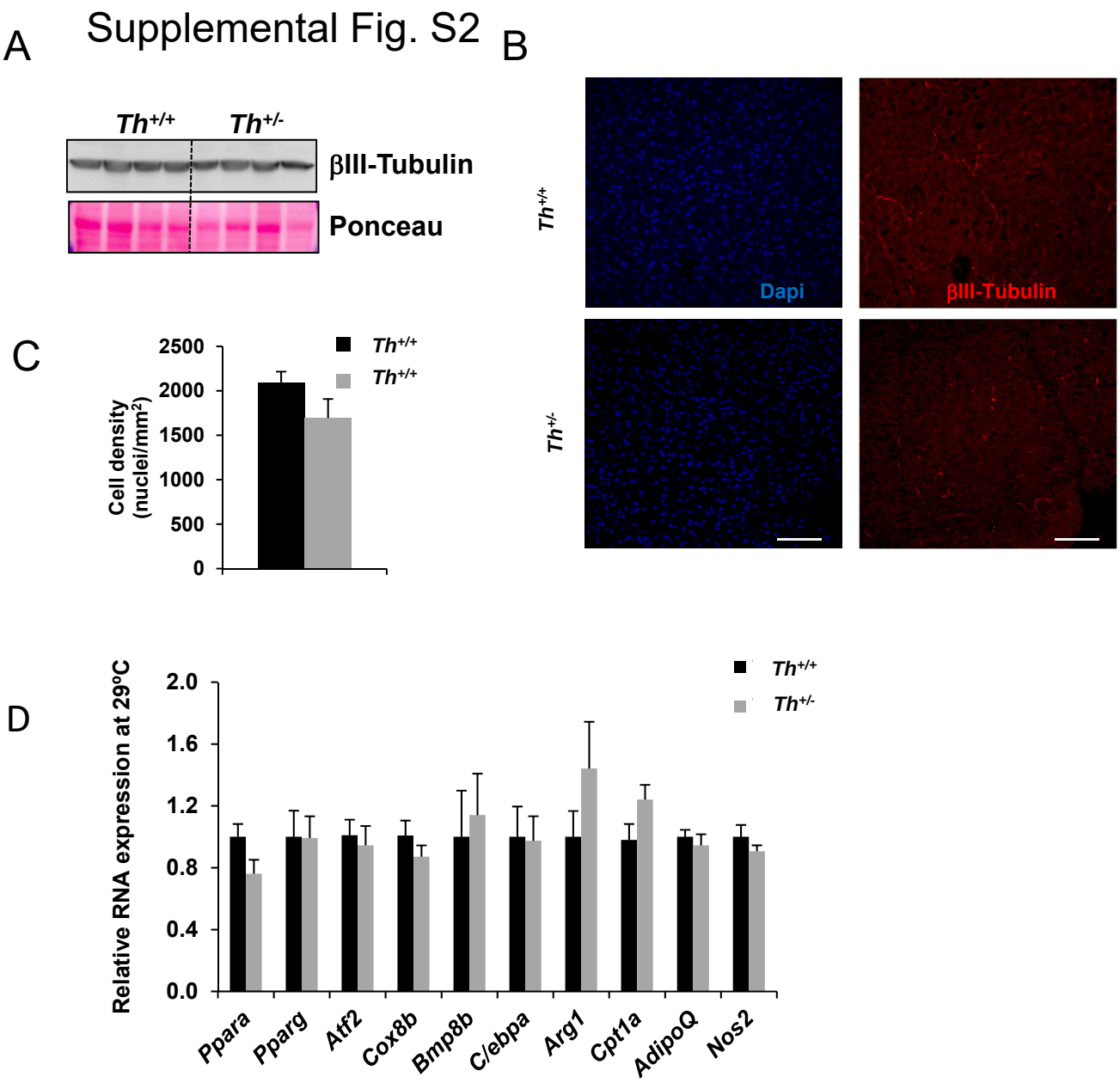

Supplemental Fig. S2. Characterizacion of BAT in thermoneutrality conditions.

A) Representative western blot of BAT extracts using β-III tubulin antibody and Ponceau stainig as a loading control. The staining of β-III tubulin fibers is shown in red. B) Representative immunohistochemistry of BAT in paraffin sections. Nuclei staining with DAPI is shown in blue. C) Quantification of nuclei/area in BAT sections stainned with H&E. D) The graphs represent the relative expression of different BAT-related genes at thermoneutral conditions. All data were relative to RNA levels of $Th^{+/+}$ mice at 29ºC. Data are mean ± SEM. n= 5-7/group in C and n= 4-11/group in D. Mann–Whitney *U* test was used. Bar scale 75µm.

Supplemental Fig. S3

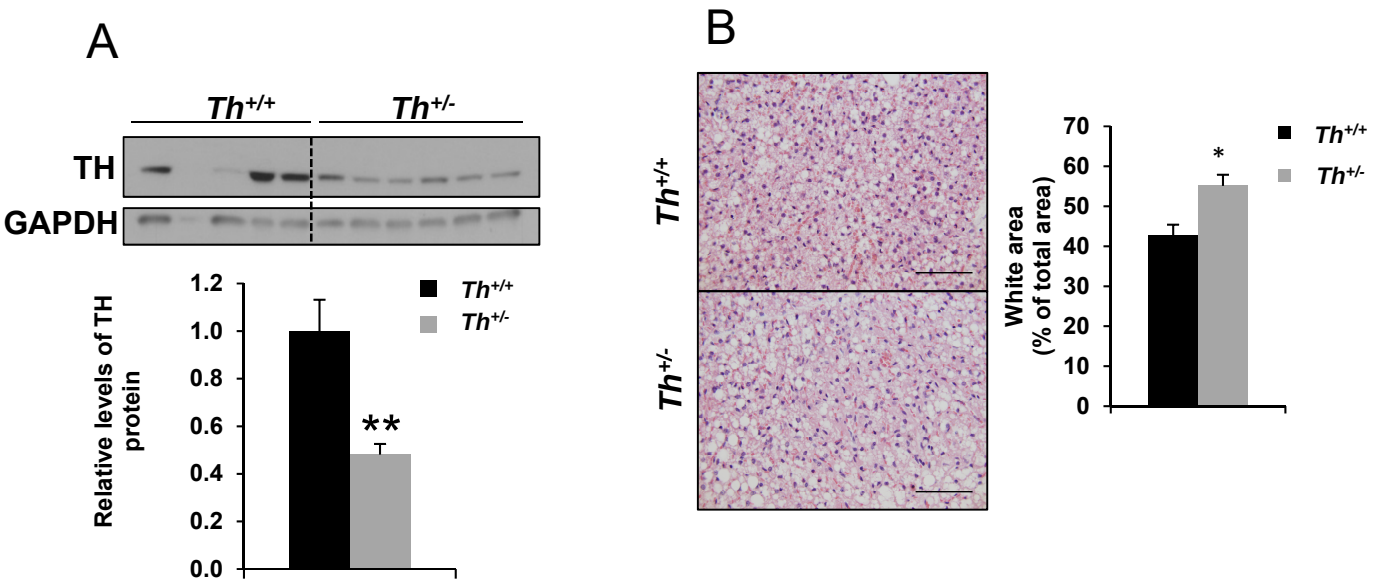

Supplemental Fig. S3. Characterization of BAT of *Th*$^{+/+}$ and *Th*$^{+/-}$ mice after cold exposure.

A) Western blot analysis and quantification of tyrosine hydroxylase (TH) in BAT lysates after cold exposure using GAPDH as a loading control. B) Representative H&E staining and quantification of white area of BAT sections of *Th*$^{+/+}$ and *Th*$^{+/-}$ mice after cold exposure. Data are mean ± SEM. n= 6-10/group in A and n= 4-5/group in B. Mann–Whitney *U* test was used. **p<0.01 between *Th*$^{+/+}$ mice and *Th*$^{+/-}$ mice group. $^{\#}$p<0.05, $^{\#\#}$p<0.01, $^{\#\#\#}$p<0.001 between each genotype at 4ºC and 29ºC group.

.

Supplemental Fig. S4

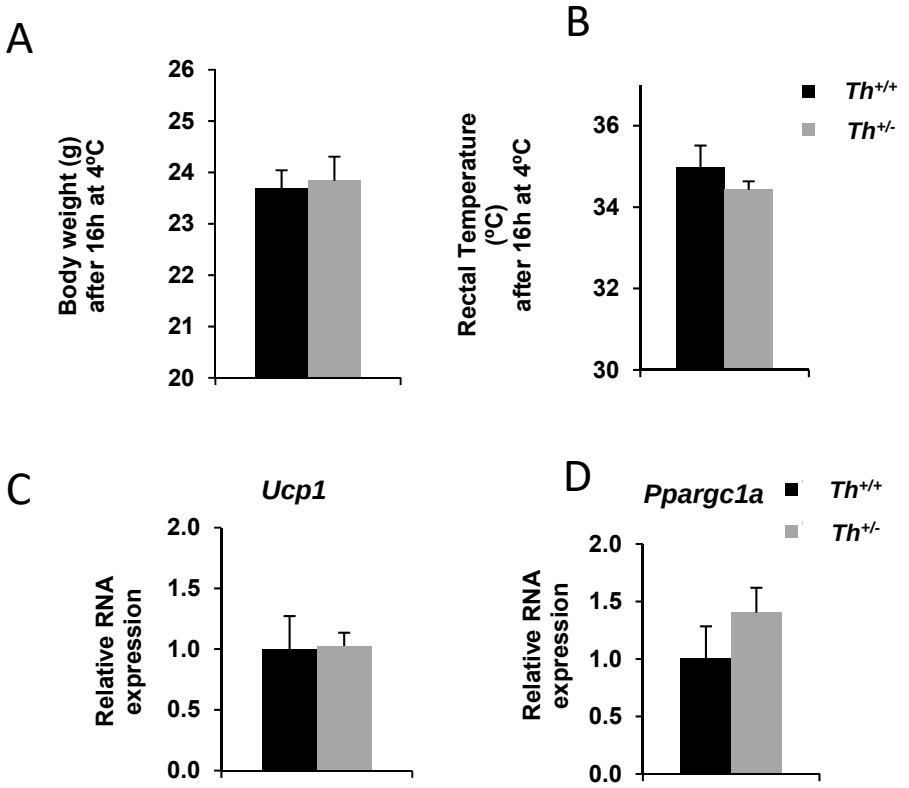

Supplemental Fig. S4. Characterization of BAT of *Th*$^{+/+}$ and *Th*$^{+/-}$ mice after 16 h of cold exposure.

A) Body weight and B) Rectal temperature were measured after 16 h of cold exposure. C-D) The graphs represent the relative expression of *Ucp1*and *Ppargc1a, r*espectively, by quantitative RT-PCR analysis in BAT after 16 h of cold exposure. Data were normalized with *Tbp* RNA expression. Data are mean ± SEM. n= 4-5/group in A and B, n= 5/group in C and D. Mann–Whitney *U* test was used.

Supplemental Fig. S5

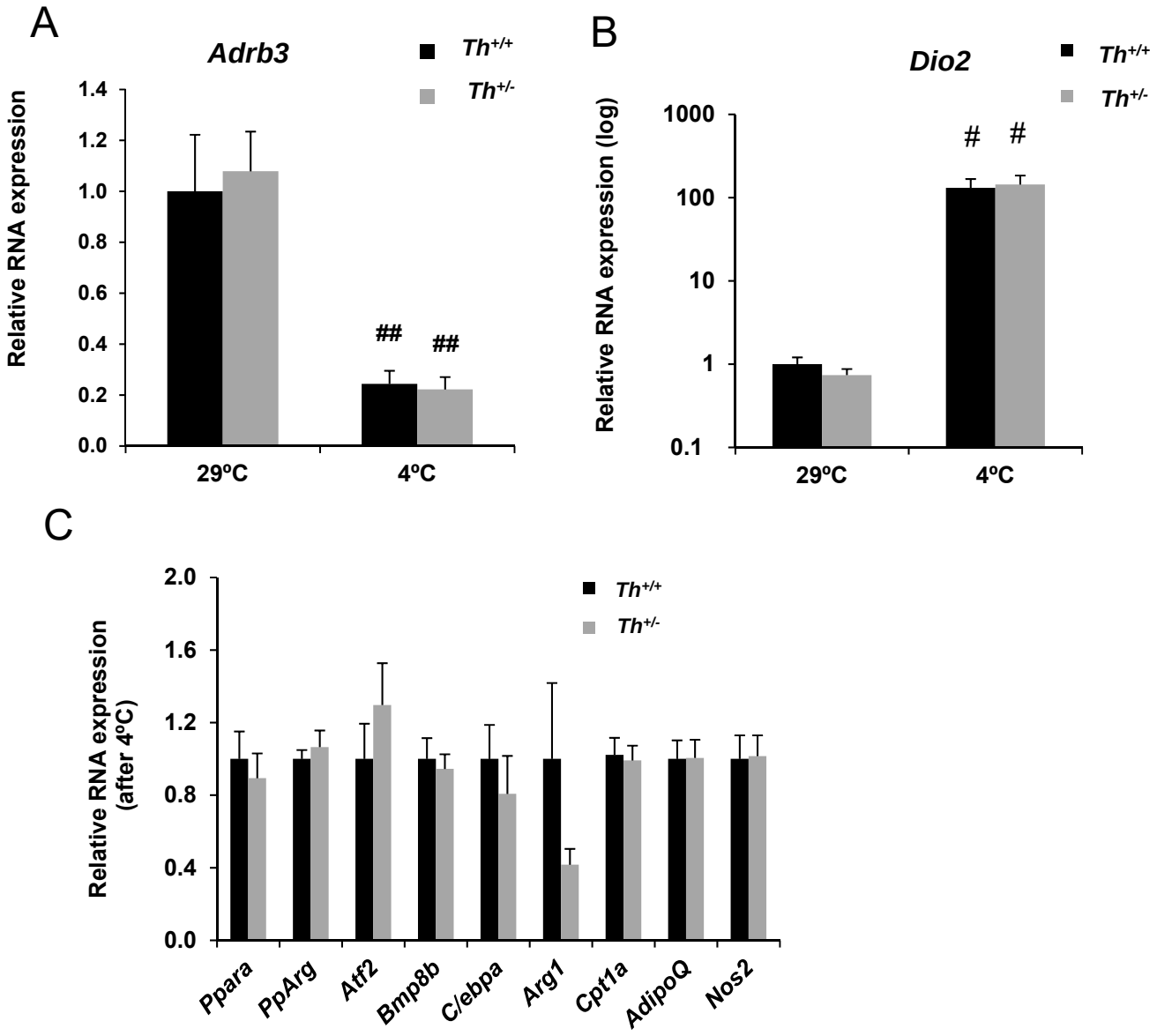

Supplemental Fig. S5. Expression of different genes in BAT of *Th*$^{+/+}$ and *Th*$^{+/-}$ mice after cold exposure. A,B) The graphs represent the relative expression of β-3-adrenergic receptors (*Adrb3*) and *Dio2 r*espectively by quantitative RT-PCR analysis in BAT. In A and B data were relative to RNA levels of *Th*$^{+/+}$ mice at 29ºC. C) The graphs represent the relative expression of several BAT-related genes. Data were relative to RNA levels of *Th*$^{+/+}$ mice at 4ºC. All data were normalized with *Tbp* or *Rlpb0* RNA expression. Data are mean ± SEM. n= 4-5/group in A and B and n=4-11 in C. Mann–Whitney *U* test was used. $^{\#}p<0.05$, $^{\#\#}p<0.01$, between each genotype at 4ºC and 29ºC groups.

Supplemental Fig. S6

A

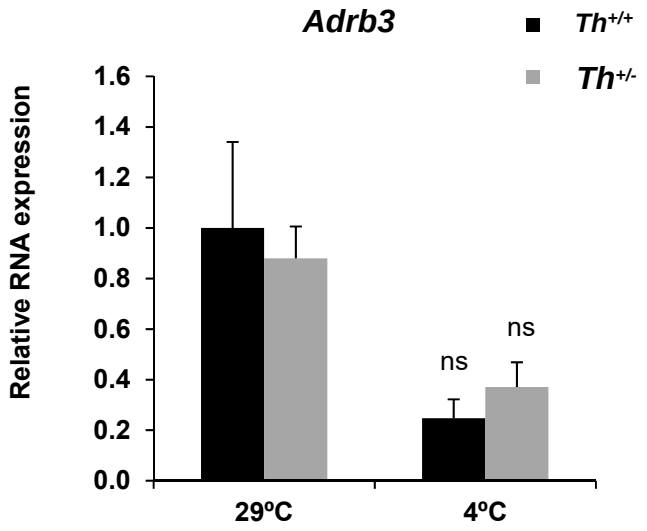

B

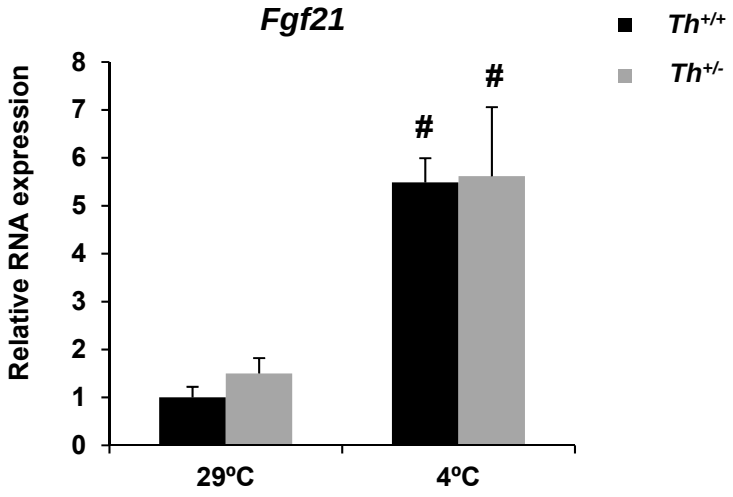

Supplemental Fig. S6. Analysis of the expression of β-3-adrenergic receptors and *Fgf21* in iWAT of *Th*$^{+/+}$ and *Th*$^{+/-}$ mice. A, B) The graphs represent the relative RNA expression of β-3-adrenergic receptors (*Adrb3*) and *Fgf21* by quantitative RT-PCR analysis in iWAT. The data were normalized with *Tbp* RNA expression. All data were relative to RNA levels of *Th*$^{+/+}$mice at 29ºC. Data are mean ± SEM. n= 3-5/group. Mann–Whitney *U* test was used. $^{\#}p<0.05$ between each genotype at 4ºC and 29ºC groups.

Supplemental Fig. S7

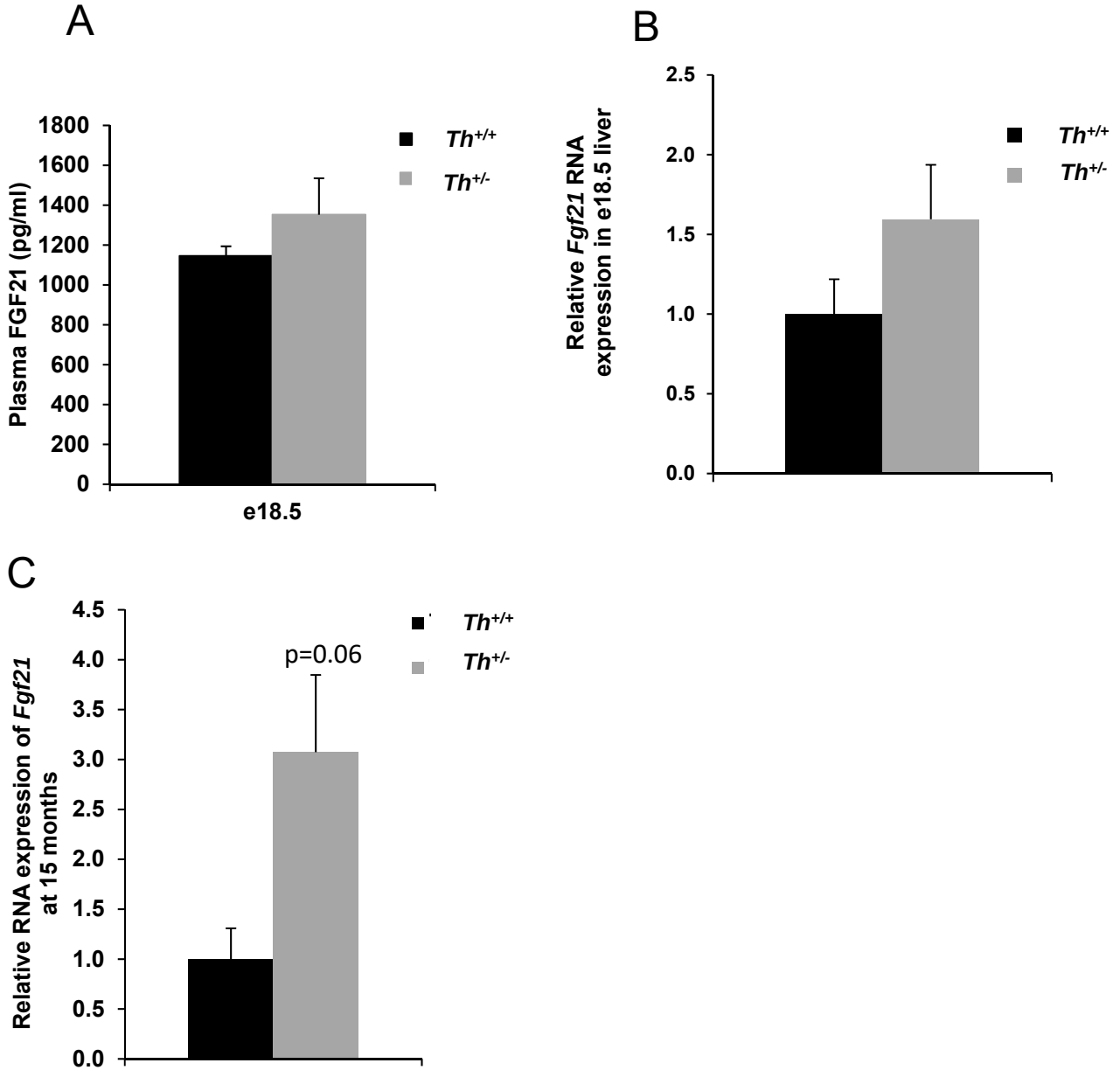

Supplemental Fig S7. FGF21 was increased in embryonic and aged *Th*$^{+/-}$ mice in basal conditions. A) FGF21 levels in plasma of e18.5 embryos. B-C) Relative expression of *Fgf21* by quantitative RT-PCR analysis in livers from e18.5 embryos and in BAT of mice at 15 months of age. The data were normalized with *Tbp* RNA expression. All data were relative to RNA levels of *Th*$^{+/+}$ mice. Data are mean ± SEM. n=4/group in A and n= 5-6/group in B and C. Mann–Whitney *U* test was used.